Synthesis of Individually Tuned Nanomagnets for Nanomagnet Logic by Direct Write Focused Electron Beam Induced Deposition

Marco Gavagnin, Heinz D. Wanzenboeck,* Domagoj Belić, and Emmerich Bertagnolli

Institute for Solid State Electronics, Vienna University of Technology, Floragasse 7/1, A-1040 Vienna, Austria

ABSTRACT Nanomagnet Logic (NML) is a promising new technology for future logic which exploits interactions among magnetic nanoelements in order to encode and compute binary information. This approach overcomes the well-known limits of CMOS-based microelectronics by drastically reducing the power consumption of computational systems and by offering nonvolatility. An actual key challenge is the nanofabrication of such systems that, up to date, are prepared by complex multistep processes in planar technology. Here, we report the single-step synthesis of NML key elements by focused electron beam induced deposition (FEBID) using iron pentacarbonyl as a gas precursor. The resulting nanomagnets feature an inner iron part and a 3 nm iron oxide cover (core–shell structure). Full functionality of conventional NML gates from FEBID-nanowires was achieved. An advanced structure maintaining the gate functionality based on bended nanowires was realized. The unique design obtained by direct-writing reduces the error probability and may merge several NWs in future NML elements.

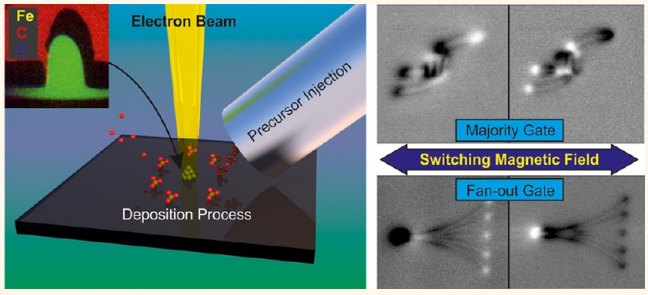

KEYWORDS: nanomagnet logic · electron beam induced deposition · iron · magnetic nanowires · nanomagnetism · computational nanotechnology

NanoMagnet Logic (NML) is a new concept for binary computation, which is attracting tremendous attention for its potential application in future computational systems.[1,2] Nowadays, further improvements in conventional chips technology based on complementary metal–oxide–semiconductor (CMOS) are limited by several issues including power consumption, energy dissipation, and down-scaling of gate dimensions.[3,4] Alternatively to charge-based conventional electronics, NML exploits magnetic interactions among nanometer-scale magnets to perform binary logic functions. This concept allows reducing the energy dissipation per switching event for a logical gate operation and eliminates the need for stand-by power, characteristics that can strongly improve the battery life in mobile information processing systems.[5]

Elongated nanomagnets such as ferromagnetic nanowires (NWs) are the key elements of the NML technology, because of the shape anisotropy that constrains the magnetization direction to a bistable state, which can encode the logic bits 0 and 1.[6] To ensure a high density packing and a controlled shape of such nanostructures, the fabrication typically has been accomplished by a multistep process including electron-beam lithography (EBL), magnetic layer evaporation, and lift-off processes.[7,8] However, many efforts are devoted to improve the nanostructure geometry beyond the capabilities of resist-based planar lithography. Significant progress was promoted by Gross *et al.* with the synthesis of nanomagnet arrays *via* nanostencil lithography, and by Becherer *et al.* using a focused ion beam to mill a previously deposited magnetic multilayer for magnetic-field coupling applications.[9,10] A hurdle of the mentioned techniques is the synthesis of structures with different heights since the evaporation/sputtering of the magnetic layer leads to a magnetic layer with homogeneous thickness.

* Address correspondence to heinz.wanzenboeck@tuwien.ac.at.

Received for review October 31, 2012 and accepted December 10, 2012.

Published online December 10, 2012
10.1021/nn305079a

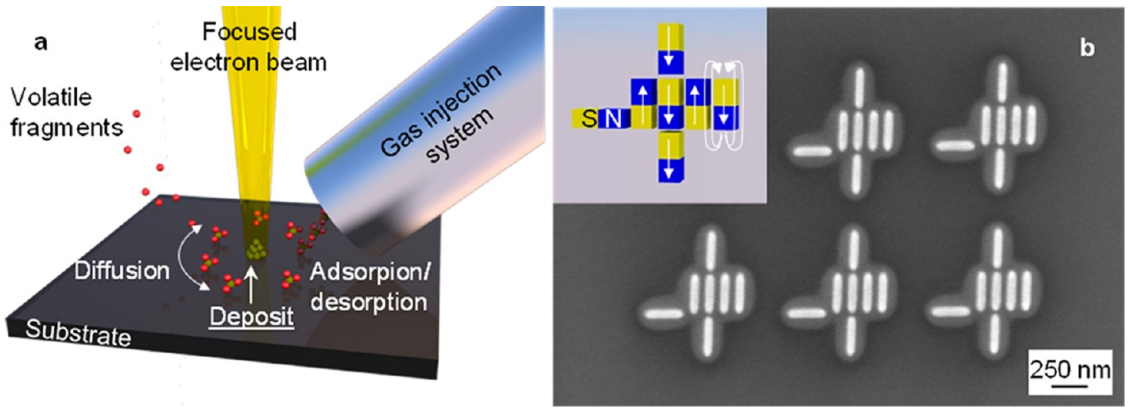

Figure 1. (a) FEBID process sketch which shows how a gas precursor is injected through a nozzle in proximity of the deposition area. A focused electron beam is promoting its decomposition and subsequent deposition, leading to a well-defined nanoscale deposit of the desired material. (b) SEM micrograph of iron nanowires fabricated by FEBID. When ferromagnetic NWs, which encode the Boolean logic, are deposited near each other, they interact through magnetic dipolar coupling (inlay) leading to processing and transport of the digital data.

As an effective improvement compared to these methods, this work, for the first time, introduces the nanofabrication of NML systems *via* focused electron beam induced deposition (FEBID). FEBID is a maskless, resistless, direct-write method which employs a focused electron beam to promote a local chemical vapor deposition process, allowing the fabrication of features with a lateral size of less than 5 nm.[11,12] This deposition technique has the unique capability to precisely define the 3-D geometry of nanosystems, with particular regard to their height. As we demonstrate in this work, the height has a strong impact on the coercitivity of the magnetic nanowires which are the key elements in NML. Furthermore, FEBID offers several other advantages like deposition on arbitrary technical substrates and on predefined areas, featuring controlled shapes of the deposit, high lateral resolution as well as *in situ* monitoring of the growth. These characteristics make FEBID an attractive alternative for the nanofabrication of devices relying on ferromagnetic materials like nano-Hall probes[13,14] magnetic force microscopy (MFM) tips,[15] domain wall-based devices,[16] and others.[17−19] Many efforts have been devoted to obtain high metal purity in FEBID magnetic nanostructures with particular regards to iron. With FEBID an iron content of 50% up to 76% has already been reported in high vacuum (HV) conditions,[20−22] and pure FEBID-Fe deposits have been obtained only in ultrahigh vacuum (UHV) conditions.[23]

In this study we evaluate the fabrication of high purity iron (>80%) ferromagnetic nanowires *via* the HV-FEBID approach for their application in digital magnet logic technology. The optimization of such nanosystems has led to second generation NML gates.

RESULTS AND DISCUSSION

Direct-writing of ferromagnetic nanowires for NML gates was performed by FEBID. Iron *penta*-carbonyl has been used as precursor for the deposition of 3-dimensional magnetic Fe structures on Si(100) by FEBID. The focused electron beam, properly guided by a pattern generator, initiates its local decomposition leading to the desired iron-based nanowires (Figure 1a,b). When these nanosystems exhibit ferromagnetic properties and are close enough to interact with each other, their magnetic dipoles will couple with the ones of the neighbors. In NML this coupling is employed for encoding and processing of digital information.

Shape and chemical composition of the deposits are the most important parameters affecting the magnetic properties of our NWs. Hence, detailed studies of geometry, especially the impact of the NW-heights, and the chemical composition were carried out by bright field transmission electron microscopy (TEM), electron energy loss spectroscopy (EELS), and energy filtered transmission electron microscopy (EFTEM). A typical cross-section of a FEBID-NW is displayed in Figure 2a. This 1 μm long NW of 153 nm height (54 scan loops) was deposited within 10 s. The TEM image shows the Si(100) substrate, the Fe-NW itself, and a dual-layer protective coating. First a thin gold protective film (~70 nm) has been thermally evaporated on the NW immediately after its FEBID fabrication. This high-purity Au film shall prevent C contamination originating from the second FEBID Pt/C layer (during the TEM lamella preparation). The Fe NW cross-section demonstrates the contribution of two different kinds of secondary electrons (SE) to the deposition process. The SE can be either produced by the primary electron beam (SE1) or by the back scattered electrons (SE2), respectively.[11,24] SE1 promoted a narrow and high deposition, corresponding to the main structure, on those areas where the primary electron beam hit the substrate surface. Around the main structure, a broad and flat deposit (base structure) is induced by the SE2. In particular, the base structure can also be promoted by the electrons scattered within the freshly deposited iron NW itself.[25]

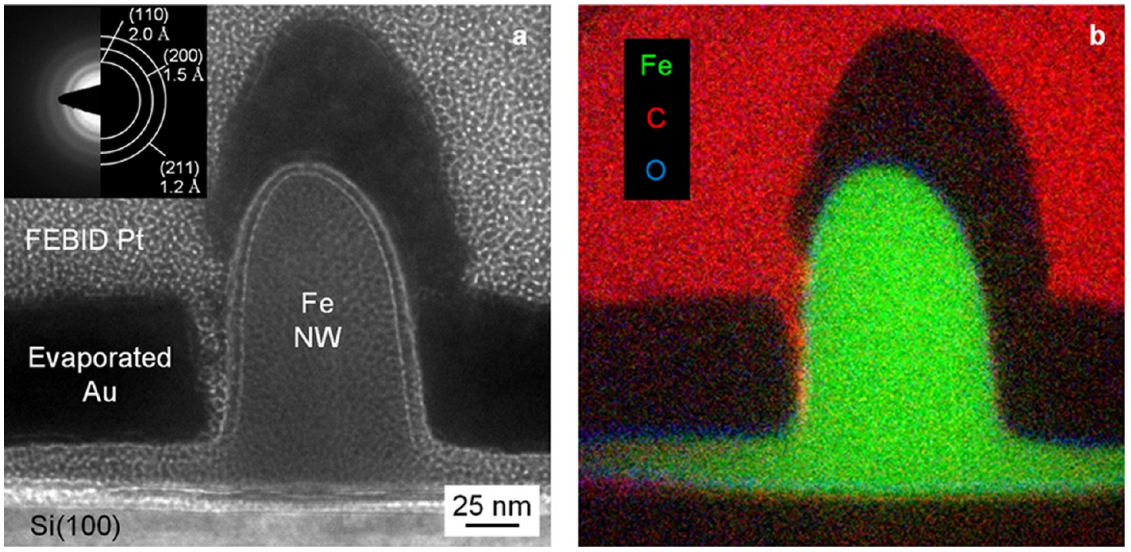

Figure 2. (a) Cross-section TEM micrograph of the 153 nm high (54 scan loops) nanowire deposited on Si(100). The two contributions of SE1 (sharp and high) and SE2 (broad and flat) on the obtained nanodeposit are evidenced. The selected-area electron diffraction (SAED) pattern of the Fe NW is displayed in the inlay, evidencing the presence of α-iron phase with crystallites size of <3 nm. (b) The corresponding EFTEM elemental map reveals the core−shell structure of the NW in which the iron inner part is completely covered by a thin layer (~3 nm) of Fe_2O_3.

The obtained morphology with a narrow peak on a broader base, resulting from the combination of the SE1 and SE2 interaction areas, plays an important role in the NML elements magnetic behavior. To comprehensively describe the magnetic properties of these systems, also the crystallinity must be taken into account. Hence, selected area electron diffraction (SAED) analyses have been performed exclusively on NWs cross sections and such a pattern is shown in the inlay of Figure 2a. The results indicate the presence of polycrystalline α-Fe phase with crystallites dimension of <3 nm. This result is not unexpected since previous work from Lavrijsen *et al*. shows the amorphous nature of this type of deposit in which small crystalline particles of α-Fe are contained.[21] To obtain compositional information from such small nanosystems, EFTEM analyses of several NWs have been executed. Figure 2b depicts the EFTEM elemental map of the above-discussed NW cross section. The atomic distribution of Fe, O, and C on the NW cross-section (Figure 2b) is a strong evidence for the presence of an iron core covered by a thin oxide layer (~3 nm), mainly constituted of Fe_2O_3, while C is uniformly distributed throughout the whole structure. The FEBID originated "core-shell" structure is ideal for the chemical stability of the system under ambient conditions, since a thin oxide layer on the NW surface passivates the Fe core and protects it from further oxidation.[26] In addition, the core chemical composition evaluated by EELS revealed an extraordinarily high Fe content of ~82%, while O and C percentages are around ~7% and ~11%, respectively. Notably, this is the first time that such a high Fe purity was achieved by FEBID fabricated Fe nanostructures under high vacuum conditions, without any substrate heating or specimen post-treatments. This result is probably due to the adopted chamber cleaning procedure based on UV irradiation in the presence of oxygen that allows us to drastically reduce the presence of carbonaceous contaminants.[27] The achieved high iron concentration in the FEBID NWs gives rise to the expectation of a magnetic behavior, which has been proved by MFM studies at room temperature (Figure 3).

In MFM the magnetic probe interacts with the magnetic forces produced by the stray fields arising from the specimen surface leading to the cantilever deflection. In Figure 3a,b topography and magnetic configuration images of a 29 nm high (9 scan loops) Fe NW deposited for 0.25 s are displayed. The investigated NWs were deposited with their long (easy) and their short (hard) axis laying on the Si substrate. The change in contrast in the phase shift images is related to the different magnetic interactions between the MFM tip and the sample surface: dark and bright contrasts are related to attractive and repulsive magnetic forces, respectively.[28] Three main regions of the fabricated nanowires can be identified by MFM (Figure 3b). In the middle part of the NW the magnetic dipoles are oriented parallel to the NW main axis and consequently cannot be detected by MFM. At both ends, on the other hand, the magnetic stray fields are clearly revealed by the change in contrast. This behavior is attributed to permanent dipole moments of iron in the NW interacting with each other. Consequently, it is reasonable to assume that the FEBID fabricated nanowires are ferromagnetic,[29] an essential property for use in NML.

Another important precondition in NML technology is the temporal stability of the ferromagnetic properties.

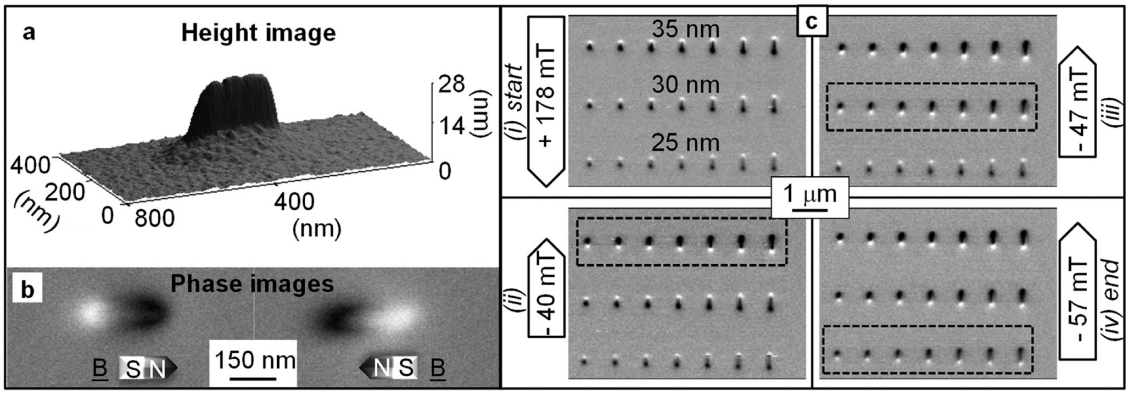

Figure 3. (a) MFM topography and (b) corresponding phase images of the NW deposited with 9 SL. The two phase images were collected after magnetization of the sample parallel to the long axis, first from left to right (left) then in the opposite direction (right). These two possible magnetic configurations represent the encoding of the Boolean logic "0" and "1". (c) Phase images showing the magnetic reversal of NWs with different lengths, from 200 to 500 nm, and heights of 25 nm (7 SL), 30 nm (9 SL), and 35 nm (11 SL). The width (FWHM) of the NWs is 105 nm (7 SL), 116 nm (9 SL), and 123 nm (11 SL). The external magnetic field applied before each measurement is shown on the side of each phase shift image, starting from +178 (*i*) to 57 (*iv*) mT. This study reveals the capability of controlling the NWs coercivity by varying the thickness.

Through MFM studies, we observed that FEBID-NWs, stored under ambient conditions, retained their magnetic configuration for several weeks, confirming the chemical stability of the core−shell structure (see Figure 2b). The magnetic configuration revealed by MFM reflects the so-called "single-domain behaviour" and it is due to the magnetic shape anisotropy of the NW.[30,31] Magnetocrystalline effects are also known to play an important role on the total free energy of a magnetic system.[32] However, since the Fe NW is polycrystalline with a very small crystallites size (<3 nm), their influence is minimal compared to the shape anysotropy in our NWs.

An essential property for the use of FEBID-NWs in NML is the possibility of programming the magnetic configuration of each of them by means of an external magnetic field (**B**). When **B** is applied parallel or antiparallel to the main NW axis (long axis), it orientates the magnetic dipoles in two opposite directions. These two possible magnetic configurations can then encode the Boolean logic "0" and "1", which in NML will be processed through magnetic coupling among neighboring NWs. Many efforts have been devoted on precisely tailoring the coercitivity of ferromagnetic NWs, in particular by designing of their lateral shape.[33,34]

As a new degree of freedom, FEBID allows not only to control the lateral dimensions (length, width) but also to vary individually the height and width of each iron nanostructure, within the same run set. An individual thickness control has a strong influence on the magnetic properties of the deposits and it allows to generate NWs with the same lateral dimension but different coercivites. In Figure 3c, MFM studies on the Fe NWs magnetization reversal, under different external magnetic fields, are reported. For initialization, in the first step the specimen was first magnetized with a high magnetic field (*ca.* +178 mT) in order to orient all the magnetic dipoles in one direction. In the succeeding magnetization steps, the external magnetic field was applied in the opposite direction, gradually increasing its magnitude (from −20 to −57 mT).

MFM studies were performed to evaluate at which strength of the switching field the NWs change their magnetic configuration in the opposite direction. For systematic studies NWs series with different lengths (from 200 to 500 nm) and height (height 25 to 35 nm) were investigated (Figure 3c). Moreover, AFM profile studies along the middle of the NWs fabricated with different SL reveal that also the full width at half-maximum (FWHM) change from 105 to 123 nm (see in S1 Supporting Information). The results of this investigation indicate that the coercivity increases with a decrease in NW thickness (height and width). This is in accordance with the mechanism of the domain-wall nucleation field since a thicker structure facilitates the magnetization reversal, hence decreasing the coercivity.[30,35]Within the tested parameter range, no trend has been observed regarding different lengths of the NWs. Moreover, the base structure created by SE2 can also be responsible for the reduced coercivity of the obtained nanosystems compared to bulk iron.[16]

The fabrication of NWs with different heights and therefore different coercivities for future NML devices enabled by FEBID is still a challenge for the conventional electron beam lithography (EBL) approach. With this conventional multistep process the desired material is deposited as a blanket layer of homogeneous thickness on the electron beam processed resist, so that the magnetic film will uniformly cover the whole substrate leading to nanoelements with same height. FEBID presents the advantage to precisely tailor the coercivity of individual magnetic NWs by means of their height.[36] This is of decisive relevance in NML for controlling their magnetic reversal to set the proper

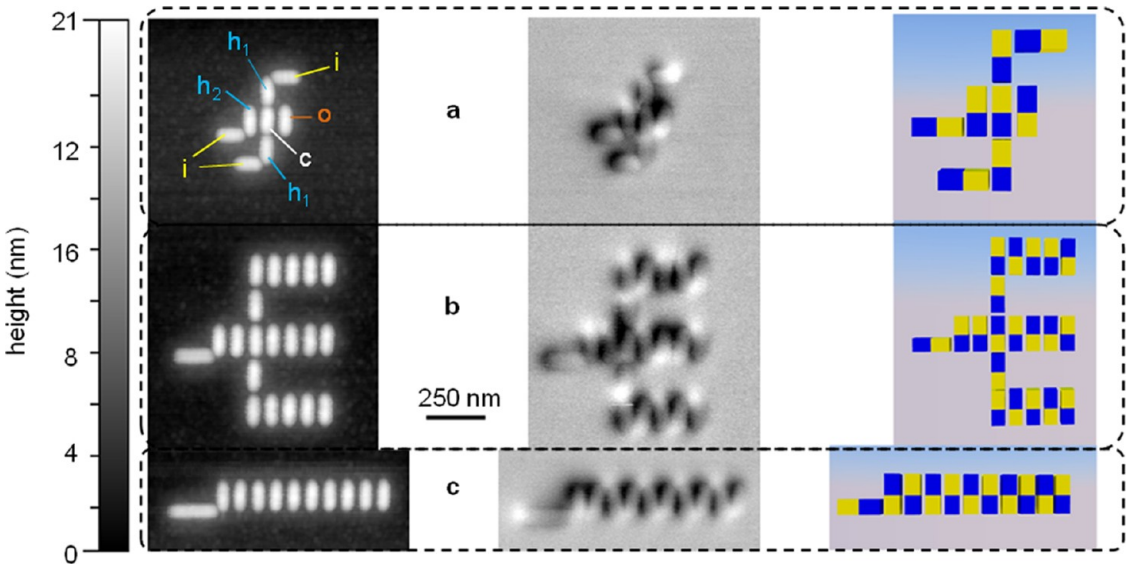

Figure 4. Topographic (left) and phase shift (center) MFM images of (a) NAND/NOR majority, (b) fan-out, and (c) information transport gates, obtained by FEBID. In particular, the majority gate is formed by a set of seven NWs: three inputs (i, yellow), three helpers (two h_1 and one h_2, blue), one central (c, white), and one output (o, red). The magnetic dipole orientations in the NWs are illustrated in the sketches on the right, in order to highlight the coupling between neighbor elements. The blue and yellow colors correspond to north and south poles respectively.

Boolean value, encoded in one of the two possible magnetic configurations.

To process the digital information we have fabricated arrays of NWs obtaining some already described NML configurations by Niemier *et al.*[5] This initial step has confirmed that NML structures with similar behavior to those realized by EBL and magnetic layer evaporation approach can be successfully obtained by FEBID. As a direct-write method FEBID allows the circumvention of masks, resists, and following lift-off processes, which are main sources of nanostructure damages. Figure 4 reports the MFM investigations executed on three different NW arrays which can perform NAND/NOR (Figure 4a), fan-out (Figure 4b), and information transport (Figure 4c) operations. This study consists of topography (height image), magnetic imaging (phase shift image), and a schematic representation of the magnetic configuration of each logic array. The digital processing is based on magnetic interactions among adjacent NWs by either ferromagnetic or antiferromagnetic coupling.[8] We will first discuss the majority gate array reported in Figure 4a, in which both of the magnetic coupling mechanisms play a key role in the logic processing. In an initial step, an external magnetic field is applied parallel to the "inputs" (i) easy axis, that is, long axis, setting their magnetization in a specific direction, while for "helpers" (h1, h2), "central" (c) and "output" (o) NWs the magnetic dipoles will orient along their hard axis, that is, short axis. Once that the external field is removed, the magnetic dipole in h_1 and h_2 will realign according to the stray fields produced by the neighbors i, setting their magnetization along their easy axis up−down (binary "1") or down−up (binary "0"). The three helpers, two h_1 and one h_2 will then couple with the central wire c by ferromagnetic and antiferromagnetic interactions, respectively, hence the majority of the helpers will set the magnetization off the central either up−down ("1") or down−up ("0"). Finally, the magnetization direction of output wire o is set by the antiferromagnetic coupling with wire c. Using this NWs configuration, it is thus possible to execute NAND/NOR computation.[37] NAND/NOR structures are relevant digital gates in logic circuits. The two possible types of magnetic couplings described above can also be used to fabricate a three-way fan-out structure (Figure 4b), an essential logic gate which allows the spread of digital information.[38] Another important process is the transport of binary information. To this aim, an array of parallel NWs along a line was fabricated. MFM results (Figure 4c) proved the successful transport of information by antiferromagnetic coupling between the NWs. Concluding, the applicability of FEBID for NML gates was successfully proven.

The main obstacles of the classic NML approach are errors in magnetic coupling between neighbor elements in arrays formed by several NWs. An example of coupling errors was observed in the fan-out gate (Figure 4b), where the magnetic dipoles orientation of many NWs is not concordant with that of the neighbors. This coupling problem is not related to the FEBID fabrication approach, since it was also found in NML circuits produced by EBL and subsequent evaporation of the magnetic layer.[39] It is worth pointing out that the discordant magnetic coupling probability is high when a large amount of nanoelements are

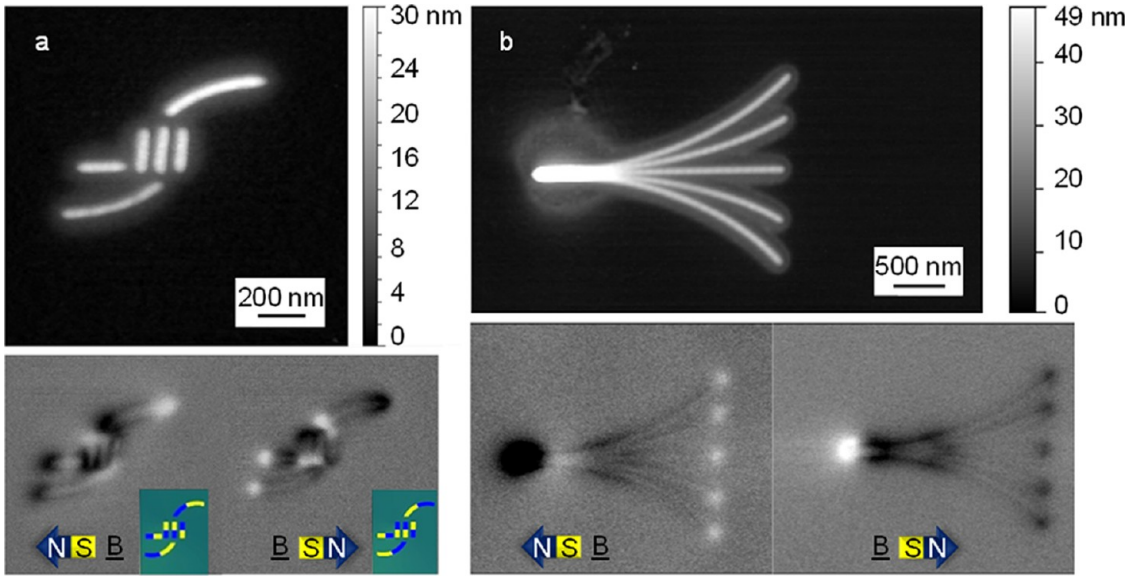

Figure 5. Topography (top) and phase shift (bottom) MFM images of the (a) NAND/NOR and (b) fanout gates fabricated by the merging of NWs. The phase shift images evidence the magnetic reversal of the gates by applying an external magnetic field in opposite directions (arrows directions), whereas the inlays in panel a, show the magnetic dipole orientations where blue and yellow represent north and south poles, respectively.

interacting with each other. Therefore, this work for the first time proposes unifying NWs in newly designed nanostructures, maintaining the gate functionality and at the same time reducing the error probability.

This work introduces "second generation" majority NAND/NOR and fan-out gates fabricated by FEBID. Regarding the NAND/NOR structure, we merged neighboring inputs i and helpers h in one single "bended wire" in order to transmit directly the proper binary information to the central wire. The central wire c is then the only one communicating with the output o (height image, Figure 5a). The simultaneous switching of all three inputs together was evidenced by applying first an external magnetic field (*ca.* +178 mT) from right to left and then the same field in the opposite direction (*ca.* −178 mT). As expected, the MFM analysis in Figure 5a (phase shift images) showed the magnetic dipoles in the central NW orientated in line with the majority of the neighbors bended inputs, and the output switched consequently.

Notably, more than 10 majority gates have been fabricated with this new configuration and no errors have been observed so far. With the fan-out gate, we managed to unify all the nanoelements in one single structure. This second generation fan-out increases the load-driving capability from three to five. At a first glance, this approach looks like a bended wire structure used for the majority gate. However, a closer look evidence, that the bended wires are all overlapping at the same input which connects all fan-out wires together (height image, Figure 5b). In this configuration the switching was proven by applying an external magnetic field on the sample in opposite directions (*ca.* ±178 mT) and, as expected, all five outputs did switch in agreement with the input (phase shift image, Figure 5b). Upon testing several fan-out gates, also in this case, we found that the error probability was drastically decreased by the bent structure.

CONCLUSIONS

We have demonstrated that iron-based (Fe > 80%) ferromagnetic nanostructures of relatively high purity can be custom fabricated by a high vacuum FEBID approach for Nanomagnet Logic technology. This nanofabrication method is a winning alternative to EBL since it is a resistless, maskless and direct-write method, leading to better defined and damage-free nanoelements. In addition, the FEBID approach opens new possibilities concerning NWs design, due to its capability of depositing nanostructures with different heights within the same run set. This exceptional advantage permits to better tailor the magnetic properties of the obtained nanodeposits, with special regard to their coercivity, leading to fine-tuning of the NWs. The design of the switching behavior is crucial for setting the proper Boolean value to different elements on the same device by means of different magnetic field magnitudes. Further studies using this approach will be performed to improve the NAND/NOR majority gate. The goal of future studies will be the individual switching of the three inputs by properly tailoring their height. Let us finally point out that we, for the first time, produced arrays of merged NWs in order to reduce magnetic coupling errors in majority (NAND/NOR) and fan-out gates. We believe that the FEBID approach will continue to contribute a

significant progress to produce second generation NML devices based on interconnected nanostructures, bringing NML technology much closer to real-world digital logic applications.

METHODS

Iron-based nanostructures were synthesized by focused electron beam induced deposition (FEBID) on Si(100) substrate starting from $Fe(CO)_5$ as gas precursor. As a standard procedure the Si substrate with ~2 nm of native oxide layer has been cleaned by ultrasonication in acetone and isopropyl alcohol directly before the deposition. The electron beam was produced by a commercial Zeiss Leo1530VP scanning electron microscope equipped with a self-built gas injection system, originally described by Hochleitner *et al.*,[17] allowing the precursor injection to the point of impingement of the focused electron beam. The precursor pressure measured in the supply line was ~2.2 mbar, which is equivalent to $\sim 3.0 \times 10^{-5}$ mbar in the reaction chamber. The base pressure in the system measured before the $Fe(CO)_5$ injection, was $\sim 2.0 \times 10^{-6}$ mbar. A focused electron beam with an acceleration voltage of 3.0 KV and 1.01 nA beam current promoted the local dissociation and subsequent deposition of the precursor molecules leading to the desired nanosystems. To fabricate nanowire arrays with high lateral precision a Raith ELPHY Plus pattern generator was employed to guide the electron beam on the substrate. The height of the deposit was controlled by the number of repetitions of electron beam scans on the same pattern (scan loop, SL): the higher the SL number is, the thicker is the resulting structure. The deposited nanostructures were characterized by TEM imaging, SAED, EELS, and EFTEM analysis using a FEI Tecnai F20-FEG transmission electron microscope. Before the TEM lamella preparation a gold protective layer was evaporated on the NWs with a Balzers PLS 500 thermal evaporation system using gold grains (>99.99%) as a precursor. MFM studies were carried out on a commercial Dimension 3100 atomic force microscope (Veeco/Bruker) using PPP-LM-MFMR magnetic tips (NANOSENSORS), which are characterized by a low momentum in order to not induce NWs reversal during the samples investigation.

Conflict of Interest: The authors declare no competing financial interest.

Supporting Information Available: Further AFM studies on the FEBID-Fe NWs width obtained with different SL. This material is available free of charge *via* the Internet at http://pubs.acs.org.

Acknowledgment. The research leading to these results has received funding from the European Community's Seventh Framework Programme (FP7/2007-2013) under Grant No. ENHANCE-238409. The authors also acknowledge the USTEM of Vienna University of Technology for the TEM.

REFERENCES AND NOTES

1. Allwood, D. A.; Xiong, G.; Faulkner, C. C.; Atkinson, D.; Petit, D.; Cowburn, R. P. Magnetic Domain-Wall Logic. *Science* **2005**, *309*, 1688–1692.
2. Wolf, S. A.; Lu, J.; Stan, M. R.; Chen, E.; Treger, D. M. The Promise of Nanomagnetics and Spintronics for Future Logic and Universal Memory. *Proc. IEEE* **2010**, *98*, 2155–2168.
3. Chau, R.; Doyle, B.; Datta, S.; Kavalieros, J.; Zhang, K. Integrated Nanoelectronics for the Future. *Nat. Mater.* **2007**, *6*, 810–812.
4. Lundstrom, M. Applied Physics: Moore's Law Forever? *Science* **2003**, *299*, 210–211.
5. Niemier, M. T.; Bernstein, G. H.; Csaba, G.; Dingler, A.; Hu, X. S.; Kurtz, S.; Liu, S.; Nahas, J.; Porod, W.; Siddiq, M.; *et al.* Nanomagnet Logic: Progress toward System-Level Integration. *J. Phys.: Condens. Matter* **2011**, *23*, 493202.
6. Kumari, A.; Bhanja, S. Magnetic Cellular Automata (MCA) Arrays Under Spatially Varying Field. *IEEE Nanotechnol. Mater. Dev. Conf.* **2009**, 50–53.
7. Pulecio, J. F.; Pendru, P. K.; Kumari, A.; Bhanja, S. Magnetic Cellular Automata Wire Architectures. *IEEE Trans. Nanotechnol.* **2011**, *10*, 1243–1248.
8. Orlov, A.; Imre, A.; Csaba, G.; Ji, L.; Porod, W.; Bernstein, G. H. Magnetic Quantum-Dot Cellular Automata: Recent Developments and Prospects. *J. Nanoelectron. Optoelectron.* **2008**, *3*, 55–68.
9. Gross, L.; Schlittler, R. R.; Meyer, G.; Allenspach, R. Magnetologic Devices Fabricated by Nanostencil Lithography. *Nanotechnology* **2010**, *21*, 425001.
10. Becherer, M.; Csaba, G.; Porod, W.; Emling, R.; Lugli, P.; Schmitt-Landsiedel, D. Magnetic Ordering of Focused-Ion-Beam Structured Cobalt-Platinum Dots for Field-Coupled Computing. *IEEE Trans. Nanotechnol.* **2008**, *7*, 316–320.
11. Utke, I.; Hoffmann, P.; Melngailis, J. Gas-Assisted Focused Electron Beam and Ion Beam Processing and Fabrication. *J. Vac. Sci. Technol., B* **2008**, *26*, 1197–1276.
12. Dorp, W. F.; van; Lazic, I.; Beyer, A.; Goelzhaeuser, A.; Wagner, J. B.; Hansen, T. W.; Hagen, C. W. Ultrahigh Resolution Focused Electron Beam Induced Processing: The Effect of Substrate Thickness. *Nanotechnology* **2011**, *22*, 115303.
13. Gabureac, M.; Bernau, L.; Utke, I.; Boero, G. Granular Co−C Nano-Hall Sensors by Focused-Beam-Induced Deposition. *Nanotechnology* **2010**, *21*, 115503.
14. Serrano-Ramon, L.; Cordoba, R.; Alfredo Rodriguez, L.; Magen, C.; Snoeck, E.; Gatel, C.; Serrano, I.; Ricardo Ibarra, M.; Maria De Teresa, J. Ultrasmall Functional Ferromagnetic Nanostructures Grown by Focused Electron-Beam-Induced Deposition. *ACS Nano* **2011**, *5*, 7781–7787.
15. Utke, I.; Hoffmann, P.; Berger, R.; Scandella, L. High-Resolution Magnetic Co Supertips Grown by a Focused Electron Beam. *Appl. Phys. Lett.* **2002**, *80*, 4792–4794.
16. Fernández-Pacheco, A.; Teresa, J.; De; Córdoba, R.; Ibarra, M.; Petit, D.; Read, D.; OBrien, L.; Lewis, E.; Zeng, H.; Cowburn, R. Domain Wall Conduit Behavior in Cobalt Nanowires Grown by Focused Electron Beam Induced Deposition. *Appl. Phys. Lett.* **2009**, *94*, 192509–192509.
17. Hochleitner, G.; Wanzenboeck, H.; Bertagnolli, E. Electron Beam Induced Deposition of Iron Nanostructures. *J. Vac. Sci. Technol., B* **2008**, *26*, 939–944.
18. Lau, Y.; Chee, P.; Thong, J.; Ng, V. Properties and Applications of Cobalt-Based Material Produced by Electron-Beam-Induced Deposition. *J. Vac. Sci. Technol., A* **2002**, *20*, 1295–1302.
19. Porrati, F.; Sachser, R.; Walz, M.; Vollnhals, F.; Steinrück, H.; Marbach, H.; Huth, M. Magnetotransport Properties of Iron Microwires Fabricated by Focused Electron Beam Induced Autocatalytic Growth. *J. Phys. D: Appl. Phys.* **2011**, *44*, 425001.
20. Shimojo, M.; Takeguchi, M.; Furuya, K. Formation of Crystalline Iron Oxide Nanostructures by Electron Beam-Induced Deposition at Room Temperature. *Nanotechnology* **2006**, *17*, 3637.
21. Lavrijsen, R.; Córdoba, R.; Schoenaker, F.; Ellis, T.; Barcones, B.; Kohlhepp, J.; Swagten, H.; Koopmans, B.; Teresa, J.; De; Magén, C.; *et al.* Fe:O:C Grown by Focused-Electron-Beam-Induced Deposition: Magnetic and Electric Properties. *Nanotechnology* **2010**, *22*, 025302.
22. Córdoba, R.; Lavrijsen, R.; Fernández-Pacheco, A.; Ibarra, M. R.; Schoenaker, F.; Ellis, T.; Barcones-Campo, B.; Kohlhepp, J.; Swagten, H.; Koopmans, B.; *et al.* Giant Anomalous Hall Effect in Fe-Based Microwires Grown by Focused-Electron-Beam-Induced Deposition. *J. Phys. D: Appl. Phys.* **2011**, *45*, 035001.
23. Lukasczyk, T.; Schirmer, M.; Steinrück, H. P.; Marbach, H. Electron-Beam-Induced Deposition in Ultrahigh Vacuum:

Lithographic Fabrication of Clean Iron Nanostructures. *Small* **2008**, *4*, 841–846.
24. Toth, M.; Lobo, C. J.; Knowles, W. R.; Phillips, M. R.; Postek, M. T.; Vladar, A. E. Nanostructure Fabrication by Ultra-High-Resolution Environmental Scanning Electron Microscopy. *Nano Lett.* **2007**, *7*, 525–530.
25. Plank, H.; Smith, D. A.; Haber, T.; Rack, P. D.; Hofer, F. Fundamental Proximity Effects in Focused Electron Beam Induced Deposition. *ACS Nano* **2012**, *6*, 286–294.
26. Shafranovsky, E. A.; Petrov, Y. I. Aerosol Fe Nanoparticles with the Passivating Oxide Shell. *J. Nanopart. Res.* **2004**, *6*, 71–90.
27. Wanzenboeck, H.; Roediger, P.; Hochleitner, G.; Bertagnolli, E.; Buehler, W. Novel Method for Cleaning a Vacuum Chamber from Hydrocarbon Contamination. *J. Vac. Sci. Technol., A* **2010**, *28*, 1413.
28. Gomez, R. D.; Luu, T. V.; Pak, A. O.; Kirk, K. J.; Chapman, J. N. Domain Configurations of Nanostructured Permalloy Elements. *J. Appl. Phys.* **1999**, *85*, 6163–6165.
29. Ashcroft, N. W.; Mermin, N. D. *Solid State Physics*; Saunders: College, 1976, pp 672−673.
30. Henry, Y.; Ounadjela, K.; Piraux, L.; Dubois, S.; George, J. M.; Duvail, J. L. Magnetic Anisotropy and Domain Patterns in Electrodeposited Cobalt Nanowires. *Eur. Phys. J. B* **2001**, *20*, 35–54.
31. Garcia, J. M.; Thiaville, A.; Miltat, J.; Kirk, K. J.; Chapman, J. N. MFM Imaging of Patterned Permalloy Elements Under an External Applied Field. *J. Magn. Magn. Mater.* **2002**, *242*, 1267–1269.
32. Ramazani, A.; Kashi, M. A.; Isfahani, V. B.; Ghaffari, M. The Influence of Crystallinity Enhancement on the Magnetic Properties of AC Electrodeposited Fe Nanowires. *Appl. Phys. A: Mater. Sci. Process.* **2010**, *98*, 691–697.
33. Niemier, M. T.; Varga, E.; Bernstein, G. H.; Porod, W.; Alam, M. T.; Dingler, A.; Orlov, A.; Hu, X. S. Shape Engineering for Controlled Switching with Nanomagnet Logic. *IEEE Trans. Nanotechnol.* **2012**, *11*, 220–230.
34. Varga, E.; Niemier, M. T.; Bernstein, G. H.; Porod, W.; Hu, X. S. Programmable Nanomagnet-Logic Majority Gate. *2010 68th Annual Device Research Conference (DRC 2010)* **2010**, 85–8686.
35. Piraux, L.; Dubois, S.; Ferain, E.; Legras, R.; Ounadjela, K.; George, J. M.; Maurice, J. L.; Fert, A. Anisotropic Transport and Magnetic Properties of Arrays of Sub-Micron Wires. *J. Magn. Magn. Mater.* **1997**, *165*, 352–355.
36. Zhong, K. H.; Zhang, Z. C.; Shen, B. H.; Lin, M. M.; Feng, Q.; Huang, Z. G. The Size and Temperature Effects of Coercivity for the Magnetic Nanowire: Monte Carlo Simulation. *Solid State Phenom.* **2007**, *121*, 1081–1084.
37. Imre, A.; Csaba, G.; Ji, L.; Orlov, A.; Bernstein, G. H.; Porod, W. Majority Logic Gate for Magnetic Quantum-Dot Cellular Automata. *Science* **2006**, *311*, 205–208.
38. Varga, E.; Orlov, A.; Niemier, M. T.; Hu, X. S.; Bernstein, G. H.; Porod, W. Experimental Demonstration of Fanout for Nanomagnetic Logic. *IEEE Trans. Nanotechnol.* **2010**, *9*, 668–670.
39. Imre, A.; Csaba, G.; Bernstein, G. H.; Porod, W.; Metlushko, V. Investigation of Shape-Dependent Switching of Coupled Nanomagnets. *Superlattices Microstruct.* **2003**, *34*, 513–518.